Princeton Plasma Physics Laboratory

PPPL- 4323

PPPL- 4323

Field-Reversed Configuration Formation Scheme Utilizing a Spheromak and Solenoid Induction

S.P. Gerhardt, E. V. Belova, M. Yamada, H. Ji,
Y. Ren, B. McGeehan,and M. Inomoto

June 2008

PPPL
PRINCETON PLASMA PHYSICS LABORATORY

Prepared for the U.S. Department of Energy under Contract DE-AC02-76CH03073.

Princeton Plasma Physics Laboratory
Report Disclaimers

Full Legal Disclaimer

Trademark Disclaimer

PPPL Report Availability

Princeton Plasma Physics Laboratory:

http://www.pppl.gov/techreports.cfm

Office of Scientific and Technical Information (OSTI):

http://www.osti.gov/bridge

Related Links:

U.S. Department of Energy

Office of Scientific and Technical Information

Fusion Links

Field-reversed configuration formation scheme utilizing a spheromak and solenoid induction

S. P. Gerhardt,[1] E. V. Belova,[1] M. Yamada,[1] H. Ji,[1] Y. Ren,[1,a)] B. McGeehan,[1] and M. Inomoto[2]
[1]*Princeton Plasma Physics Laboratory, Plainsboro, New Jersey 08543, USA*
[2]*Osaka University, Osaka 565-0871, Japan*

(Received 8 January 2008; accepted 6 February 2008; published online 26 March 2008)

A new field-reversed configuration (FRC) formation technique is described, where a spheromak transitions to a FRC with inductive current drive. The transition is accomplished only in argon and krypton plasmas, where low-n kink modes are suppressed; spheromaks with a lighter majority species, such as neon and helium, either display a terminal tilt-mode, or an $n=2$ kink instability, both resulting in discharge termination. The stability of argon and krypton plasmas through the transition is attributed to the rapid magnetic diffusion of the currents that drive the kink-instability. The decay of helicity during the transition is consistent with that expected from resistivity. This observation indicates a new scheme to form a FRC plasma, provided stability to low-n modes is maintained, as well as a unique situation where the FRC is a preferred state. © *2008 American Institute of Physics*. [DOI: 10.1063/1.2889428]

I. INTRODUCTION

Compact toroidal (CT) plasmas,[1] which include the spheromak[2–4] and field-reversed configuration (FRC),[5] share a number of unique features. These include a very low aspect ratio, a lack of toroidal field coils linking the plasma, and a natural divertor geometry. Possible applications for these plasmas include the burning core of a fusion power plant,[6,7] a fueling scheme for large tokamak facilities,[8–11] and basic science studies of highly self-organized plasmas.[12–15]

A key area of research in CT plasmas is the formation of the configuration. The formation of spheromak plasmas has been demonstrated via many different methods,[4] including flux-cores,[16] coaxial plasma guns,[17] combined theta- and Z pinches,[18] conical theta-pinches,[19] kinked Z pinches,[20] and steady inductive helicity injection (SIHI).[21] The formation of axially elongated FRC plasmas has, however, been limited to rotating magnetic fields,[22] fast formation by theta-pinch coils,[5] and in a single case, a scheme known as the Coaxial Slow-Source.[23,24] Formation of oblate (more spherical) FRC plasmas has generally been limited to the merging of spheromaks,[25–28] or in a single case, a laser produced plasma coupled to fast coil ramps.[29,30] Finding additional formation techniques for FRC plasma could potentially expand the usefulness of the configuration for basic and applied plasma science research. In this paper, we report a new and unique means to form a FRC plasma, and describe situations where this might be a preferred formation technique.

Another area of CT research studies the very different equilibrium properties of the two configurations. For instance, the plasma current in a spheromak is dominantly parallel to the magnetic field, while the current is largely perpendicular to the field in a FRC. The spheromak equilibria has been widely understood in terms of a MHD relaxation principal, from both a theoretical[31,32] and an experimental[17,33–35] perspective. Two-fluid relaxation principles have been proposed for understanding FRC equilibria,[36,37] and some experimental evidence for such high-β relaxed states has been reported.[38,39] In this paper we report a configuration where the spheromak is not the preferred state, even though the plasma begins as one. By stabilizing the low-n kink instabilities for longer than the current decay time, while continually injecting poloidal flux via solenoid induction, a spheromak is naturally transformed into a FRC.

In the magnetic reconnection experiment (MRX),[40] the dynamic transition from a spheromak to a FRC equilibrium has been observed, when inductive current drive is applied to the spheromak. The transition only occurs when the current drive is applied to argon and krypton spheromaks, which display stability to low-n kink instabilities. The transition does not occur in spheromaks formed in helium or neon; as q_0 drops below 1/2 in these cases, a large $n=2$ mode grows which terminates the plasma. The decay in helicity during the transition is consistent with Ohmic dissipation. MHD simulations with the HYM code[41] indicate that the low-n stability in heavy ion species plasmas is likely due to the low Lundquist number in these cases. This scheme provides insight into the physics of (CT) plasmas, and may provide a simplified technique for forming FRCs in some contexts.

The outline for the remainder of this paper is as follows. A description of the relevant background physics is contained in Sec. II, and the MRX facility as configured for these experiments is described in Sec. III. A brief description of unstable spheromaks in helium and neon is given in Sec. IV. A detailed description of the spheromak to FRC transition is given in Sec. V, and the role of resistivity in stabilizing $n=2$ kinks is discussed in Sec. VI. A discussion and summary concludes the paper in Sec. VII. Note that a brief summary of this work was presented in Ref. 42.

[a)]Present address: University of Wisconsin-Madison, Madison, Wisconsin 53706, USA.

II. BACKGROUND: THE ROLE OF STABILITY IN DIFFERENTIATING SPHEROMAK AND FRC EQUILIBRIA

The spheromak equilibrium is usually understood by the Taylor equilibrium relationship,[32] $\vec{\nabla}\times\vec{B}=\lambda\vec{B}$ with the Taylor eigenvalue λ a spatial constant related to the parallel current density. This equilibrium condition results naturally from minimizing the total magnetic energy at fixed magnetic helicity $K=\int\int\int\vec{A}\cdot\vec{B}dV$. The Taylor equilibrium condition implies that all currents are parallel to the magnetic field, the pressure gradient is zero (or small[43]), and the volume average β is low ($\beta=2\mu_0\int nTdV/\int B^2dV$ with n and T the plasma temperature and density, B the magnetic field and $\int\ldots dV$ the integral over the plasma volume). This spheromak equilibrium naturally leads to a toroidal configuration where the toroidal field has a maximum at the center of the plasma and goes to zero at the edge, while the poloidal field is maximized at the plasma edge and zero in the center.

The maintenance of this equilibrium state is typically related to low-n MHD modes, where n is the toroidal mode number. For instance, in high-performance discharges in the S-1 spheromak,[34] the toroidal field, which is produced by currents at the cooler plasma edge, decayed more quickly than the poloidal field, which was produced by currents in the hot plasma core. This differential decay led to a drop in both the edge λ and central safety factor (q_0). However, when q_0 dropped beneath $1/2$, an $n=2$ internal kink mode developed. This kinking and subsequent relaxation lead to the conversion of poloidal flux to toroidal flux,[35] and thus to the restoration of the flat λ profile with $q_0>1/2$. Similar behavior was observed in simulation,[44] and relaxation oscillations were observed in CTCC-1 (Ref. 45) and in the Compact Toroid Experiment (CTX, Ref. 46).[47] In the SPHEX (Ref. 48) and Sustained Spheromak Physics Experiment (SSPX, Ref. 49) devices, both of which are gun-driven spheromaks, an $n=1$ mode appears to be related to the maintenance of the Taylor equilibrium.[50,51]

The pure FRC equilibrium, on the other hand, has only poloidal magnetic field and toroidal plasma current. This toroidal plasma current is purely diamagnetic [$\vec{J}_\perp=(\vec{B}\times\nabla p)/en$], leading to a configuration with β approaching one, but helicity and Taylor eigenvalue equal to zero. These FRC configurations are predicted to be unstable to a variety of pressure-driven instabilities,[52–56] due to their high-β, everywhere bad curvature, and lack of magnetic shear. It has been proposed that high-n modes may be responsible for maintaining the FRC equilibrium in a state of marginal stability.[56]

The FRC and spheromak equilibria have traditionally been thought of as two distinct branches of the compact toroid family. This distinction has been supported by spheromak counter-helicity merging research in the Tokyo Spheromak (TS)-3/4 devices. A series of experiments in TS-3 utilized counter-helicity merging to find conditions where the plasma after merging would relax to a FRC.[14] It was found that if the two spheromaks were well balanced (i.e., the toroidal fields, though oppositely directed, had closely matched magnitudes), then the toroidal field after merging would be near zero and a FRC equilibria would result. However, for unbalanced merging, there would be residual toroidal field after the merging. An $n=2$ mode often grew in the unbalanced case, leading to flux-conversion and relaxation to a spheromak. A MHD-like criterion was found for the threshold for relaxation to a FRC, based on the sum of the Taylor eigenvalues of the initial spheromaks compared to the expected spheromak eigenvalue. Research on the larger TS-4 device showed that relaxation to a FRC after counter-helicity merging only reliably occurred when the initial spheromaks were formed in a heavy working gas.[15] It was hypothesized that some two-fluid physics must play a role in allowing the relaxation.

However some recent results from prolate FRCs have blurred this distinction. In the translation, confinement, and sustainment (TCS) experiment, theta-pinch formed FRCs translating from the formation region into a confinement chamber have been observed to contain large toroidal fields.[38] After multiple bounces off of magnetic mirrors in the confinement chamber, the plasma settled in a new equilibrium with smaller but still substantial toroidal field. Substantial toroidal fields were also observed in FRCs formed by rotating magnetic fields (RMF).[39] In this case, poloidal currents driven by the RMF generated toroidal field in the plasma core. The toroidal and poloidal field profiles near the poloidal field null resembled those of a spheromak equilibrium, providing evidence of a high-β FRC equilibrium with a low-β spheromaklike central region.

III. THE MRX FACILITY

The Magnetic Reconnection Experiment (MRX),[40] which is illustrated in Fig. 1, is a flexible facility with the capacity to study both the basic science of magnetic reconnection and the physics of compact toroid plasmas. In the latter studies, the currents in the two flux-cores are programmed such that each flux-core produces a spheromak[16]; the two spheromaks are then allowed to merge by the attractive force of their parallel currents, as well as pushing forces from the flux-cores. This paper focuses on cases where the two initial spheromaks have parallel toroidal fields, so that the configuration resulting from merging is a further spheromak (i.e., "co-helicity" merging); when the two spheromaks have oppositely directed toroidal field, the resulting configuration is that of a FRC ("counter-helicity" merging). A 68 turn solenoid, composed of two separate 34 turn coils, one on either side of the midplane, is installed along the geometric axis of the device. This coil is utilized to apply an inductive toroidal electric field to the plasma once merging is finished, and thus sustain the toroidal current of the CT. The coils are contained within a 0.13 mm thick inconel vacuum liner. The solenoid was powered by a 420 μF capacitor bank, which was charged to at most 11 kV during the CT inductive sustainment campaign; the two solenoids were always connected in series for this set of experiments, resulting in the longest possible solenoid current ramp. An additional pair of compensation coils was present in the vacuum vessel, with two independent turns in each coil. One winding in each coil was connected in series with the solenoids to cancel the re-

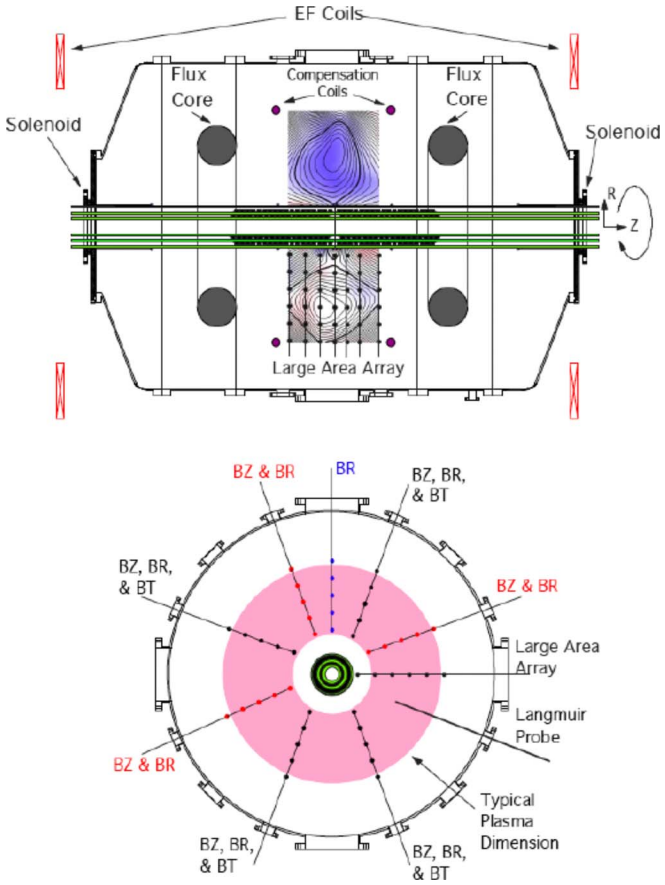

FIG. 1. (Color online) Schematic of the MRX device, illustrating the spheromak-forming flux-cores, compensation coils, solenoids, and major diagnostics utilized in this research. The measured poloidal flux (contours) and toroidal field (colors) of typical FRC and spheromak discharges are superimposed on the top figure.

turn flux of the solenoids and thus preserve radial equilibrium. The other winding of each coil was connected in series with the flux cores, in order to improve the field curvature in a way similar to that described in Ref. 28. Hence the total "vertical field" present to maintain the radial equilibrium of the plasma is the sum of that from the large dc "EF" coils, the flux-cores, the compensation coils, and the return flux from the solenoid.

The main diagnostics utilized in this study are two large arrays of magnetic pickup coils. One array, known as the large area array, is composed of 7 linear magnetic probe arrays in the $R-Z$ plane, spaced by ~8 cm in the axial direction. Each individual linear array has three-component magnetic field sensors at 6 locations radially separated by 8 cm. This probe array, when combined with measurements of the solenoid flux from loops on the vacuum liner surface, is utilized to determine the spatially and temporally resolved equilibrium properties, assuming axisymmetry. These include the toroidal and poloidal currents, the poloidal flux, the toroidal flux, and the toroidal electric field as

$$J_T = \frac{1}{\mu_0}\left(\frac{\partial B_Z}{\partial R} - \frac{\partial B_R}{\partial Z}\right), \tag{1}$$

$$\vec{J}_P = \nabla\phi \times \nabla\left(\frac{RB_T}{\mu_0}\right), \tag{2}$$

$$\psi = 2\pi \int_{R_{\text{solenoid}}}^{R} RB_Z dR + \psi_{\text{loop}}, \tag{3}$$

$$\Phi = \int\int_{\psi<\psi_{\text{sep}}} B_T dA, \tag{4}$$

$$E_\phi = \frac{1}{2\pi R}\frac{d\psi}{dt}. \tag{5}$$

Here, ψ_{loop} is the initial condition for the radial integration provided by the solenoid flux loops. These quantities in turn allow a calculation of the Taylor eigenvalue (λ) and safety factor (q). The trapped poloidal flux, ψ_t, is defined as the poloidal flux at the separatrix minus the poloidal flux at the poloidal field null ($\psi_t = \psi_{\text{Sep}} - \psi_0$).

The second set of probes, known as the "spoke probe array," consists of 8 probes inserted at approximately equally spaced toroidal angles at the midplane. Each probe can measure all three components of the magnetic field at five radii separated by 8 cm. The measured magnetic field is typically Fourier decomposed at each time point and radius into cosine and sine components with amplitudes $C_n(R,t)$ and $S_n(R,t)$,

$$B(R,\phi,t) = B_0(R) + \sum_{n=1}^{n_{\text{Max}}} [C_n(R,t)\cos(n\phi) + S_n(R,t)\sin(n\phi)], \tag{6}$$

where B can be any of B_R, B_T, and B_Z. However, due to digitizer channel number limitations, not all 135 coils were recorded. Sufficiently many channels were digitized from this array to measure B_R up to $n=4$, B_Z up to $n=3$, and B_T up to $n=2$ (one probe in the large area array also contributed data to the spoke probe array). The time response was limited by the bandwidth of the integrators to about 3 μs. Note that the $n=0$ components from this array were utilized to calculate the poloidal flux in most figures in this paper. This is useful when large instabilities lead to nonaxisymmetries that cause the large area array data to be unrepresentative of the average configuration.

IV. MHD UNSTABLE SPHEROMAKS UNDER INDUCTIVE CURRENT DRIVE

Free-boundary spheromaks are often unstable to an $n=1$ instability known as the tilt[57] mode. This mode is caused by the tendency of the spheromak to align its magnetic moment to the external magnetic field. The typical method for eliminating the tilt is to place the plasma in an appropriately sized flux-conserver.[2] Alternatively, the external field can be configured to have curvature such that $n_{\text{decay}} = -(R/B_Z)dB_Z/dR > 1$.[58] The external field in the preset experiments typically had $n_{\text{decay}} = 0.5-0.6$ near the spheromak magnetic axis immediately after merging. Once the solenoid current ramp began, the external field was dominated by the solenoid/compensating field combination, which

produced $n_{decay} > 1$. Hence, the plasma configuration became more stable to the tilt as the solenoid was ramped. Spheromak tilting has been observed in many experiments,[58–60] including a previous attempt at inductive sustainment of a spheromak;[61] our result agrees with the latter study in that the tilt instability absolutely terminated the sustainment. The tilt instability was the dominant feature of all deuterium, most helium, and many neon spheromaks. These tilting plasmas will not be discussed further in this paper. Note that other techniques have been suggested in the past in order to stabilize the tilt, including figure-8 coils[58,62] and "dipole trapping."[60]

A diligent exploration of the available operating space found plasma regimes where the tilt instability was reliably suppressed. These plasmas typically had larger fill pressure (8–10 mT in neon, marginal suppression at >14 mT in helium), with strong external field pushing the plasma toward the solenoid. It is likely that the slower growth rate at higher density, possible coupled to some line-tying to the liner, assisted in forming this comparatively stable regime. Also note that the radial-shift instability was not observed in this tilt-free case, even through simulation[63] and analytic theory[64] have indicated that this shifting mode is *typically* unstable when the tilt is stable. The observed stability to the shift is likely related to the complicated external field structure around the spheromak in a fashion similar to the stability reported in Ref. 28. However, no specific numerical calculations of shift or tilt growth rates were done to confirm this hypothesis.

This tilt-free regime in neon is illustrated in the solenoid capacitor bank voltage scan (0, 3, 5, 7, and 9 kV) in Fig. 2, where each curve is the average over 3–4 repeatable discharges. The gray area on the left of the plot indicated the period before the merging is finished. Frame 2a shows the solenoid flux, as measured by the loops on the solenoid surface, for the different discharges in the scan. The trapped poloidal flux is shown in Fig. 2(b) for these discharges. The inductive current drive always leads to some extension of the plasma lifetime, and can even increase the poloidal flux when fired with sufficiently high voltage. The toroidal flux, however, shows in Fig. 2(c) a monotonic decline as the poloidal plasma currents decay. The decline in the toroidal field leads to a reduction in central safety factor (q_0), which eventually passes through 1/2. It is at this moment that the $n=2$ midplane magnetic perturbation in Fig. 2(e) begins to grow. This mode eventually leads to the termination of the configuration. The growth rates for these $n=2$ modes will be discussed in greater detail below.

The expected value of the Taylor eigenvalue can be estimated by considering the prediction for a cylindrical flux conserver,[65]

$$\lambda_{cyl} = \sqrt{\left(\frac{3.83}{r_c}\right)^2 + \left(\frac{\pi}{h}\right)^2}. \quad (7)$$

Here, r_c is the radius of the flux conserver and h is the height. Utilizing $h=0.35$ m and $r_c=0.4$ m, we estimate $\lambda_{cyl}=13$. A similar estimate, based on a spherical flux conserver,[57] yields $\lambda_{sph}=4.49/R_c=11$, where R_c is the radius of the conserver and has been approximated by 0.4 m. The measured "global" Taylor eigenvalue, defined as $\lambda_G=\mu_0 \int J \cdot BdV / \int B \cdot BdV$ and plotted in Fig. 2(c), shows a slight increase in time as the configuration shrinks ($\lambda \propto 1/R$), but always stays in the range expected for a spheromak Taylor equilibrium.

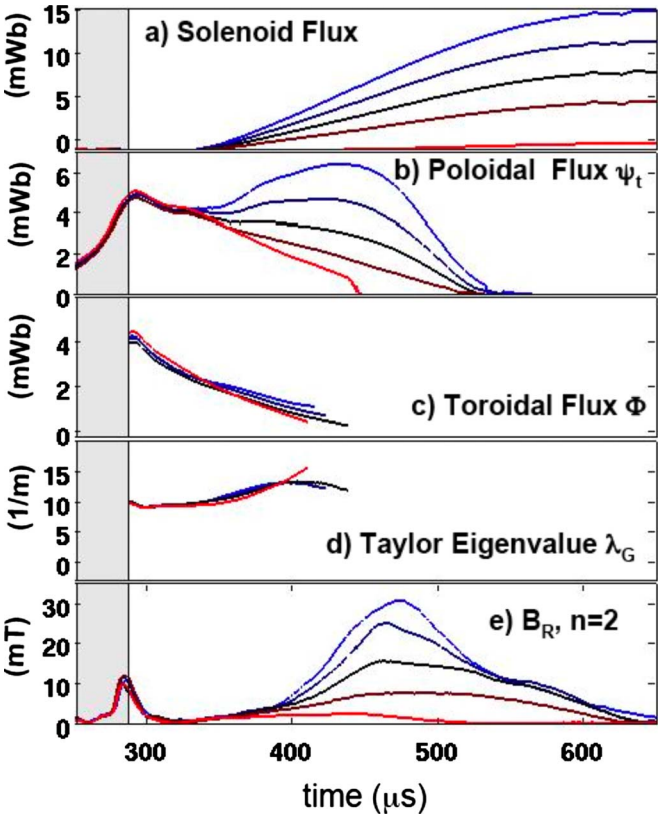

FIG. 2. (Color online) Evolution of neon spheromaks under inductive sustainment. The grey area corresponds to time before merging is complete.

These $n=2$ modes show a distinct similarity to those observed in S-1,[34,35] with the important difference that the plasma in the present case is disrupted. S-1 had nearby passive conductors in the form of figure-8 coils and conical stabilizers, which presumably provided this stability. In the present case without nearby passive stabilizers, the $n=2$ mode always leads to the termination of the discharge.

V. CONVERSION FROM A SPHEROMAK TO A FRC

This unstable behavior is in stark contrast to the behavior reliably observed in argon (and krypton). Figure 3 shows the poloidal flux (contours) and toroidal field (colors) for two typical argon discharges: One with inductive sustainment (top row) and one without (bottom row). In both cases, the co-helicity merging is complete at $t=280$ μs, and the plasma has settled as a large spheromak by $t=320$ μs. From this point forward, the spheromak toroidal flux resistively decays in both cases. The poloidal flux decay, however, is arrested when the solenoid system is energized at $t=350$ μs, after which the poloidal flux is slightly increased and then sustained. The configuration thus transitions to a FRC equilibrium by $t=440$ μs. This final state is not dissimilar to that

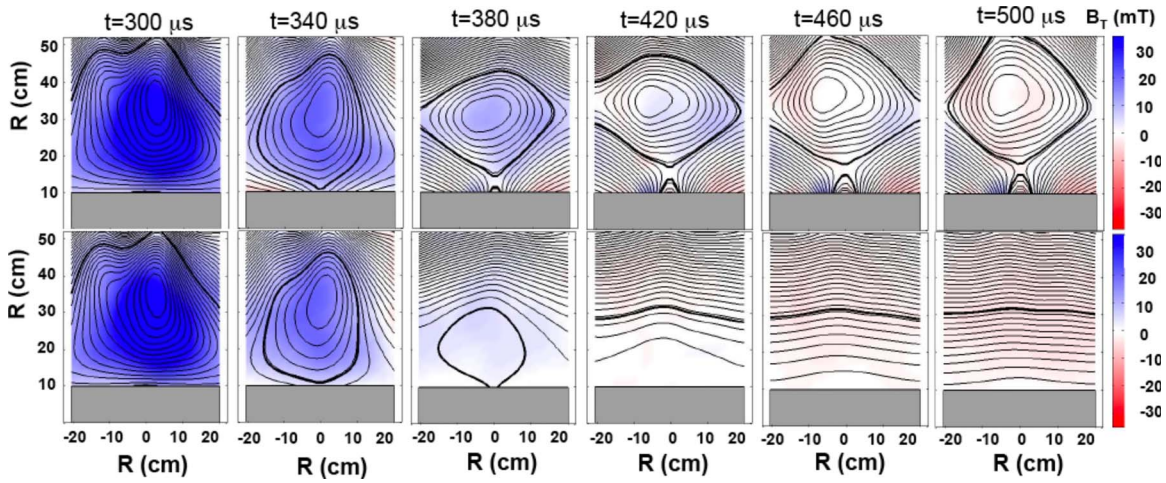

FIG. 3. (Color online) Two-dimensional measurements of the poloidal flux (contours separated by 0.35 mWb) and toroidal field (colors, in millitesla) for argon spheromaks with (upper row) and without (lower row) inductive sustainment. The upper plasma transition from a spheromak to a FRC. The grey area at the bottom of each figure is the location of the solenoid coil.

which would have occurred if inductive current drive had been applied to a FRC initially formed by counter-helicity merging

Figure 4 illustrates the profiles of the toroidal magnetic field (top row), poloidal field (middle row), and midplane electron pressure (bottom row), for sustained (closed symbols, Solenoid capacitor bank voltage of 8 kV) and unsustained (open symbols) discharges. The light grey shaded areas represent the approximate locations of the inboard and outboard plasma boundaries at the midplane. The B_Z and B_T profiles are those of a typical spheromak at 340 μs, and the electron pressure is not centrally peaked, but rather increases toward a small major radius. This density profile is likely caused by a strong particle source on the surface of the solenoid. The solenoid current ramp begins at that time, leading to a steady maintenance of the poloidal fields in the sustained case. The toroidal fields, however, continue to decay throughout the period. At 460 μs, the unsustained case has totally decayed away (the small positive toroidal field is due to residual poloidal plasma currents, probably driven by ringing in the flux core circuits, and decays to zero at a later time). The sustained case, however, has completed its transition to an equilibrium with significant poloidal but virtually no toroidal field, i.e., it is a FRC. This transition is accompanied by the formation of a peaked pressure profile, as expected for the diamagnetic FRC equilibrium, due mainly to a rise in the plasma density. This FRC state is then sustained for the remainder of the solenoid current ramp. Given that the purpose of this paper is to document the spheromak →FRC transition, the subject of FRC sustainment will not be discussed further; a detailed description of inductively sustained FRCs is given in Refs. 66 and 67.

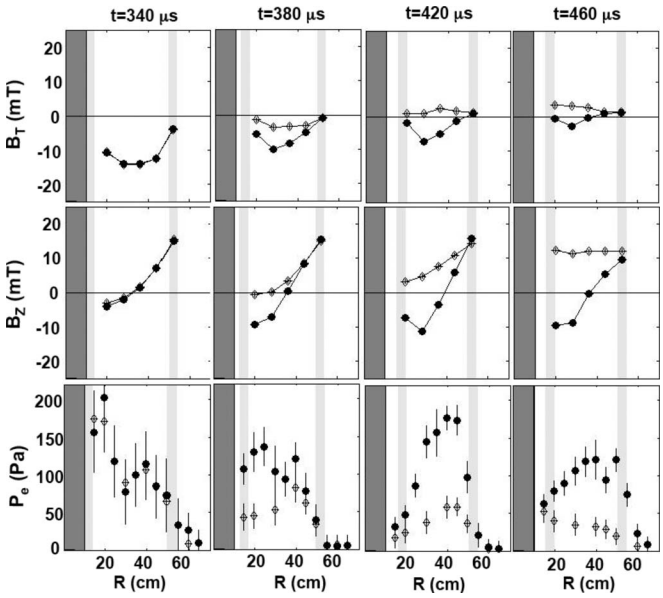

FIG. 4. Evolution of the midplane profiles, for argon spheromaks that are allowed to decay (open symbols), and which transition to a FRC via inductive current drive (closed symbols). The toroidal field (top row), poloidal field (middle row), and electron pressure (bottom row) are illustrated.

This transition is observed to be quite robust in argon, and quite distinct from the behavior in neon and helium. As an example, the results of an solenoid capacitor bank voltage scan in argon are plotted in Fig. 5. The quantities plotted are the same as in Fig. 2, and on the same scale; the voltages in the scan (V_{OH}=0, 3, 5, 7, 9) are also the same. These argon examples illustrate a robust response to the inductive drive, with the trapped poloidal flux either sustained or even increased by the solenoid current ramp. The toroidal flux in Fig. 5(c), however, continues to decay, eventually going to zero in all cases. Note that the toroidal flux decay is largely independent of the solenoid power supply voltage; it is this separation of the toroidal and poloidal flux evolution that allows the robust transition to a FRC. The value of q_0 goes through many $1/n$ resonances during this transition, yet the data in Fig. 5(e) shows that there is no discernible n=2 mode growth during these discharges; the n=1, 3, and 4 perturbations to B_R are also small throughout the transition. Hence, the behavior of these plasmas is apparently two-dimensional.

The robustness of the transition is further indicated by

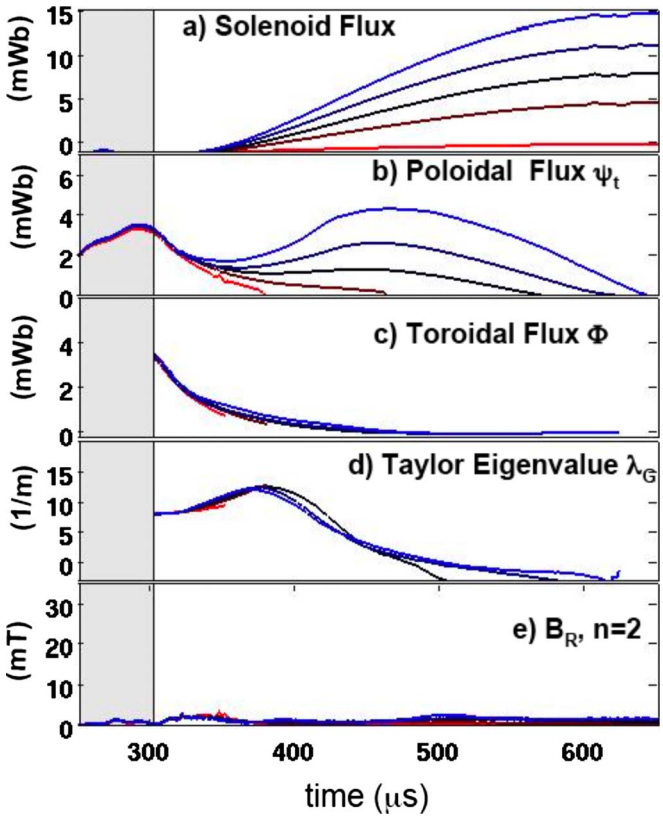

FIG. 5. (Color online) Time evolution of argon spheromaks with different solenoid firing voltages. The scan and quantities plotted are identical to those in Fig. 2, but with argon instead of neon.

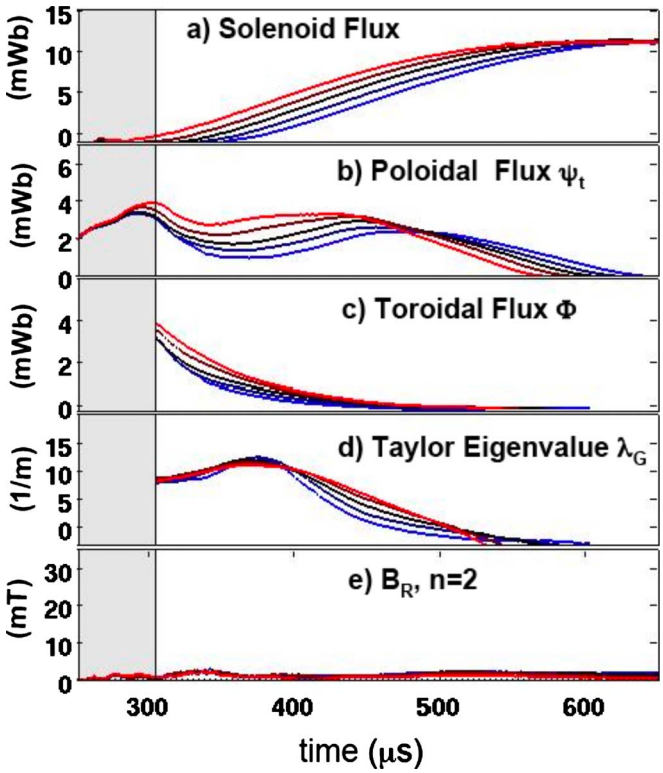

FIG. 6. (Color online) Time evolution of argon spheromaks with different starting times for the solenoid current ramp.

the results of a scan over the solenoid firing time at fixed power supply voltage, shown in Fig. 6. The scan was conducted to understand if ramping the solenoid early in the discharge, before a substantial fraction of the toroidal flux had decayed away, could lead to the sustainment of a spheromak equilibrium. The solenoid current ramp began just after merging completion in the earliest cases, as demonstrated in Fig. 6(a). The poloidal flux was maintained throughout this current ramp in all cases. This early timing did lead to a moderately longer period of spheromaklike equilibrium, indicating that the solenoid system was indeed injecting some helicity into the system (as will be discussed below). This is indicated by the somewhat longer period of λ_G near the spheromak level in the early current-ramp cases. Ultimately, however, all cases showed the transition to a FRC equilibrium. In no case were strong low-n modes observed.

Other scans not shown here have further demonstrated the robustness of this phenomenon. When the argon fill pressure is scanned at fixed solenoid power supply voltage and timing, the transition is always observed to occur. Reversing the toroidal fields of the two initial spheromaks has no result on the dynamics of the transition. Spheromaks formed in krypton ($M=84$) show similar transition characteristics.

The dynamics of this transition are further illustrated by examining the profiles of $\lambda(\psi)=\mu_0\langle J\cdot B\rangle/\langle B\cdot B\rangle$, where $\langle\ldots\rangle$ implies an average over the magnetic surface. Figure 7 illustrates these profiles for sustained and decaying plasmas, for both an argon case which illustrates the transition and a neon case which develops an $n=2$ instability. The profiles are plotted against a radial coordinate $\rho=\sqrt{V/(2\pi^2R_0)}$, where V is the volume inside the magnetic surface, and R_0 is the major radius of the plasma. There is a slightly hollow λ profile immediately after merging ($t=310$ μs), likely because the toroidal reconnection current during merging is in the direction opposite to the toroidal current of the spheromaks. This profile relaxes to a flat λ profile, as expected for low-T_e spheromaks with no external drive,[2] and with a value (~ 11 m^{-1}) that is appropriate for the physical size of the plasma. The effect of the inductive sustainment becomes visible at 340 μs. The λ profile then becomes highly peaked in the sustained cases, due to a peaking of the parallel current density on the axis. For the argon case, the profile then drops to zero throughout the volume as the poloidal currents decay away (the large error region near the axis is because $B=0$ on the axis of a FRC). This completes the transition to a FRC. As noted above, the neon case develops a large $n=2$ mode during the period of peaked λ, leading to the termination of the discharge.

This transition from a spheromak to a FRC represents a transition from a state with net magnetic helicity to one with no helicity. The evolution of helicity can be understood from the helicity balance equation,[68]

$$\frac{dK}{dt}=2\Phi V_\phi-2\int \vec{E}\cdot\vec{B}dV. \tag{8}$$

The gauge-invariant helicity is defined as[68,69]

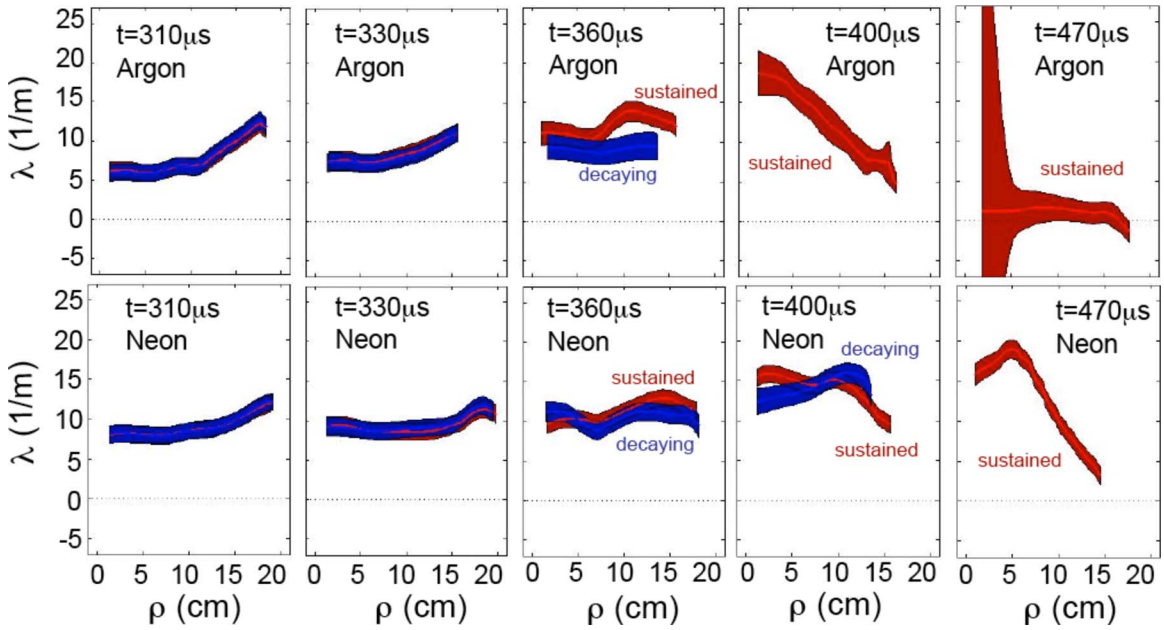

FIG. 7. (Color online) Comparison of the λ profiles in sustained and decaying discharges, for argon (top row) and neon (bottom row) discharges.

$$K = \int \Phi d\psi + \int \psi d\Phi - \Phi(a)\psi_{\text{sep}}. \tag{9}$$

The first term on the RHS of Eq. (8) represents the injection of helicity, and requires that there be (toroidal) flux aligned with the toroidal electric field from the solenoid; this term is equal to zero in a FRC state with no toroidal field. The second term on the RHS is the helicity dissipation rate. We have computed an effective resistivity based on the helicity dissipation (η_K),[70] by using the parallel Ohm's law $E=\eta J$ in the helicity balance equation. The resulting resistivity is defined as

$$\eta_K = -\frac{\frac{dK}{dt} - 2\Phi V_\phi}{2\int \vec{j}\cdot\vec{B}dV}. \tag{10}$$

The results of the calculation are illustrated in Fig. 8. Figure 8(a) illustrates the time evolution of the toroidal, poloidal, and solenoid fluxes, showing again that the toroidal flux decays to zero while the poloidal flux is sustained. Figure 8(b) shows the magnetic helicity, which decays in time, going to zero long before the (sustained) poloidal flux decays. The resistivity determined from Eq. (10) is illustrated in Fig. 8(c). Also shown is the Spitzer parallel resistivity[71] ($\eta_\parallel = 0.5\times10^{-4}T_e^{-3/2}Z_{\text{eff}}\ln\Lambda$), assuming $Z_{\text{eff}}=1.5$ (note that many collisional plasmas in MRX have resistivities near the collisional value[72,73,67]). The value of T_e in this calculation comes from a triple Langmuir probe, which was located at $R=0.35$ m during these experiments. The resistivities agree to within a factor of 2, with overlapping error bars. Furthermore, the parallel resistivity, estimated as the ratio of the central toroidal electric field to the central current density during the spheromak phase, lies approximately between these curves. We thus infer that the helicity decay is likely simply due to collisional resistivity. Unfortunately, given the uncertainties in the helicity-balance terms, and the error in the Spitzer resistivity measurement (especially the assumed Z_{eff}), more detailed comparisons between the resistivities are not possible.

VI. SPHEROMAK STABILITY UNDER INDUCTIVE CURRENT DRIVE

The understanding of this transition revolves around the stability of the $n=2$ kink in these argon and krypton plasmas. The electrical resistivity plays a key role in suppressing the $n=2$ kink instability in these cases. When the plasma is sufficiently resistive, the perturbed currents that drive the instability are dissipated more quickly than the instability can grow. They key parameter is then the ratio of the resistive time to the Alfvén time, known as the Lundquist number, and defined as $S=\mu_0 a V_A/\eta$ with $V_A=B_{Z,\text{sep}}/\sqrt{\mu_0\rho}$, a the minor radius, $B_{Z,\text{sep}}$ the B_Z field at the outer separatrix, and ρ is the mass density. For sufficiently small values of S, the instability is expected to be suppressed. Note that the equilibrium toroidal currents are sustained by the solenoid induction for periods much longer than the resistive decay time.

In order to test this hypothesis, we have conducted simulations of the spheromak $n=2$ mode growth with the MHD portion of the HYM code.[41] A Taylor equilibrium spheromak with a $q=1/2$ surface in the plasma was formed, and the $n=2$ kink allowed to grow from the numerical noise. The inductive sustainment was simulated by eliminating the $n=0$ component of the resistivity, while keeping resistivity for the perturbations. The simulation was repeated for various values of the resistivity, thus forming a scan over S. The growth rate is normalized to the inverse Alfvén time $\gamma_A = 1/\tau_A = V_A/a$.

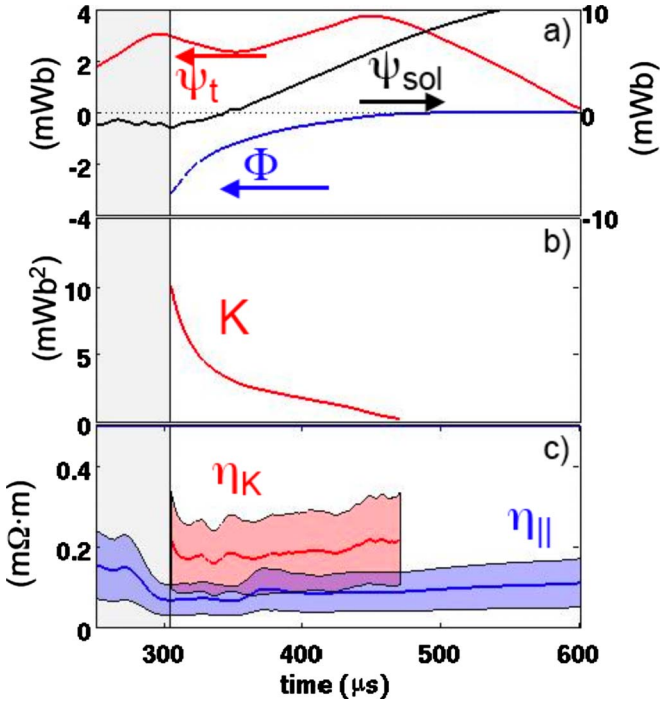

FIG. 8. (Color online) Analysis of magnetic helicity balance. (a) The toroidal (Φ), trapped poloidal (ψ_T), and solenoid (ψ_{sol}) fluxes; (b) the magnetic helicity; and (c) the resistivity inferred from helicity balance (η_k) and the parallel Spitzer resistivity ($\eta_{||}$). The arrows in (a) indicate which vertical axis is associated with each curve.

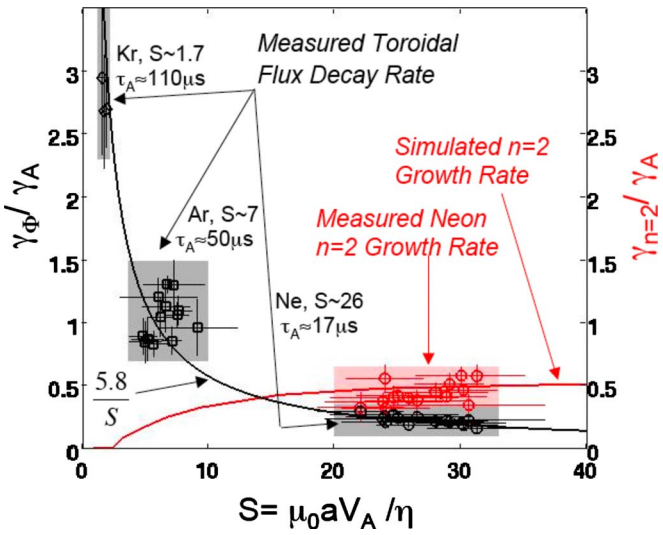

FIG. 9. (Color online) Comparison of the $n=2$ growth rate ($\gamma_{n=2}$) from HYM and measurements in neon plasmas, and the toroidal flux decay rate (γ_Φ), as a function of the Lundquist number.

The results of these simulations, along with comparisons to measurements, are illustrated in Fig. 9. These simulations show a decreasing $n=2$ growth rate as S is decreased, ultimately leading to stability for $S<2.5$. The $n=2$ growth rate in neon plasmas was estimated by fitting an exponential curve to the measured $n=2$ midplane perturbation growth. The $n=2$ mode was observed to grow at a rate of $\gamma_{n=2}/\gamma_A \approx 0.5$, in good agreement with the numerical prediction. No $n=2$ mode growth was observed in the krypton and argon plasmas, and hence none is plotted.

The decay rate of the toroidal flux is also plotted for the neon, argon, and krypton plasmas. This decay rate is calculated by fitting the observed toroidal flux evolution to an expression of the form

$$\Phi(t) = \Phi_0 e^{-\gamma_\Phi (t-t_0)}, \tag{11}$$

where Φ_0, γ_Φ, and t_0 are fit parameters. The decay rates have been normalized to the same inverse Alfvén time as the $n=2$ growth rates. These rates are plotted for the three gases in black symbols in Fig. 9. For neon, the $n=2$ mode grows approximately twice as fast at Φ decays. Hence, only a fraction of the toroidal flux will have decayed before the $n=2$ mode disrupts the plasma. In contrast, the toroidal flux in argon and krypton decays much faster than the $n=2$ mode can grow, and the transition is allowed to occur.

The normalized toroidal flux decay rate shows a clear 5.8/S dependence, as indicated by the black hyperbola in Fig. 9. This is exactly the scaling expected from magnetic diffusion. Ignoring the convective term, the toroidal field decay is described by the diffusion equation[74]

$$\frac{\partial B_\phi}{\partial t} = \frac{\eta}{\mu_0}\nabla^2 B_\phi. \tag{12}$$

The cylindrical solution of this equation satisfying the boundary condition $B_\phi = 0$ at the edge is given by

$$B_\phi(r,t) = B_{\phi,0} J_0\left(\frac{2.4r}{a}\right) e^{-\gamma_D t} \tag{13}$$

with $\gamma_D = 5.8\eta/(\mu_0 a^2)$. J_0 is the zeroth order Bessel function, which also happens to be the lowest order solution for the toroidal field in a Taylor equilibrium in a straight cylinder.[31] Utilizing the definition of S provided above, and assuming that the decay rate of the toroidal flux (γ_Φ) is similar to the decay rate of the field (γ_D), the ratio of the diffusion rate to the Alfvén growth rate can be estimated as

$$\frac{\gamma_\Phi}{\gamma_A} = \frac{5.8\eta}{\mu_0 a^2}\frac{a}{V_A} = \frac{5.8}{S}. \tag{14}$$

This scaling shows excellent agreement with the measurements.

Even though we have stressed the role of resistivity in the present experiments, it is important to note that the key feature in this process is not the Lundquist number per se, but rather the suppression of the kinklike instabilities. In the case described here, this stability is indeed provided by the resistive dissipation of the perturbation currents. However, any other mechanism outside of the ideal MHD that might provide stability (shear flow, finite-Larmor radius stabilization, etc.) might also facilitate this transition. The only essential role of resistivity is to dissipate the poloidal currents that generate the spheromak toroidal field.

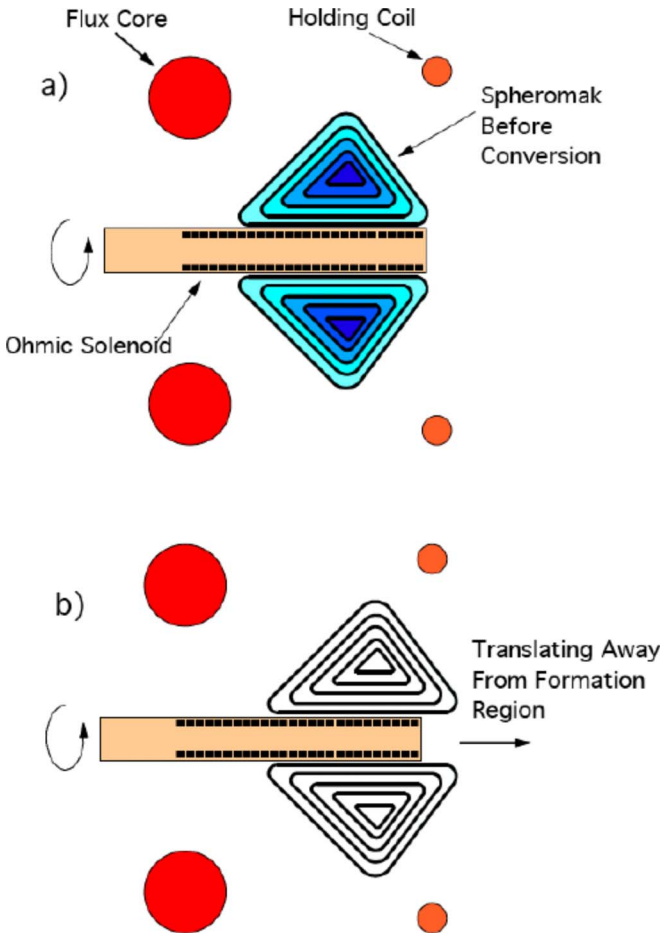

FIG. 10. (Color online) Schematic illustration of FRC formation utilizing only a single flux-core and a solenoid.

VII. DISCUSSION

The technique described here may have certain advantages for forming high-density, resistive, oblate FRCs, compared to the merging scheme traditionally utilized in MRX,[28] TS-4,[15] and the Swarthmore Spheromak Experiment (SSX).[27] In particular, it allows for the formation of a FRC utilizing only a single flux-core, along with a single solenoid. In this formation scenario, the solenoid is initially "charged" with current. A single spheromak is formed around the solenoid, most likely using a flux-core. As shown schematically in Fig. 10(a), the spheromak is held in place during the solenoid current ramp between the "holding-coils" and the toroidal windings of the flux-core, both of which have currents opposite the toroidal plasma current. The solenoid current is then ramped down, applying a toroidal loops voltage and allowing the transition to occur. The current in the "holding-coils" is then ramped down, allowing the FRC to translate away from the flux-core into a simply connected confinement volume [Fig. 10(b)]. Note that the flux-core current will contribute to the pushing force for the translation, and that the precharging of the solenoid eliminates any stray solenoid field during the translation. The FRC can then be utilized for whatever studies are envisioned.

There are many possible advantages to this scheme. It eliminates the additional power supplies, high voltage feedthroughs, and vacuum seals associated with one of the flux-cores, simplifying the system design. Additionally, given sufficiently large power supplies and a robust solenoid, very high levels of FRC flux could be achieved by this means. Furthermore, the spheromak merging process can be quite violent and unstable,[28] and avoiding this might be advantageous in some contexts. If this hardware were duplicated on the opposite side of the vacuum chamber, a FRC merging experiment could be constructed. In terms of flexibility, this scheme provides a single "black box" plasma source for producing either high-β FRCs or low-β spheromaks, depending on whether the solenoid is energized, but without hardware modifications. Such a scheme could be beneficial for the SPIRIT (Ref. 75) FRC concept.[76]

This scheme for FRC formation may also have drawbacks. One advantage of spheromak merging is the large reconnection heating, as the energy in the toroidal fields of the FRC is converted to plasma kinetic and thermal energy.[77] The present scheme clearly does not have this feature. However, the resistive decay of the poloidal currents should lead to some Ohmic heating,[78] which may mitigate this downside. We also note that the utility of this scheme is dependent on the ability to prevent Taylor relaxation. In the present argon case, the relaxation is prevented by the resistive diffusion of the perturbed magnetic field. In higher-S plasmas, Taylor relaxation should be more robust, and other effects outside of standard ideal MHD are surely needed in order to prevent relaxation. We hypothesize that properly driven shear-flows could possibly stabilize the kink,[79,80] as might finite-Larmor radius effects if an energetic neutral beam were injected in the plasma. These hypotheses remain to be tested by experiment and theory.

The observations in this paper also suggest an instance where the preferred plasma state is a FRC. This occurs when the kinklike instabilities are suppressed for a time longer than the resistive decay time, yet poloidal flux is externally fed into the system. The toroidal flux can then smoothly decay to zero without triggering an instability, and the final sustained plasma will be a FRC.

Once the plasma has transitioned to a FRC state, it should, as noted above, be susceptible to pressure-driven instabilities. Many of the stabilizing effects mentioned above (equilibrium field shaping and magnetic diffusion) likely play a role in the continued stability of the configuration after it becomes a FRC, and finite-Larmor radius effects[81] are stronger in a FRC, due to the large region of small field. The sustainment and stability of oblate FRC plasmas has been discussed in separate publications.[66,67]

In summary, the transition from a spheromak to a FRC equilibrium has been observed, when inductive current drive is applied to an argon spheromak. The transition was quite robust in argon and krypton, though kink and tilt instabilities terminated the configuration when lighter gases (He, Ne) were used. This transition represents a unique way to form a FRC.

ACKNOWLEDGMENTS

The authors would like to thank Dave Cylinder for assistance constructing the diagnostics used in these experiments, Robert Cutler for assistance with all aspects of maintaining and upgrading the MRX facility, and Yasushi Ono for valuable discussions. The PPPL technical staff, including Don McBride, Doug Loesser, Jim Chrzanowski, Frederick Simmonds, Frank Terlitz, and Mike Hauss, were instrumental in the design and construction of the solenoid system.

[1] H. P. Furth, J. Vac. Sci. Technol. **18**, 1073 (1981).
[2] T. Jarboe, Plasma Phys. Controlled Fusion **36**, 945 (1994).
[3] P. M. Bellan, *Spheromaks, A Practical Application of Magnetohydrodynamic Dynamos and Plasma Self-Organization* (Imperial College Press, London, 2000).
[4] T. R. Jarboe, Phys. Plasmas **12**, 058103 (2005)
[5] M. Tuszewski, Nucl. Fusion **28**, 2033 (1988).
[6] M. Kutsurai and M. Yamada, Nucl. Fusion **22**, 1407 (1982).
[7] H. Momota, A. Ishida, Y. Kohzaki, G. H. Miley, S. Ohi, M. Ohnishi, K. Yoskikawa, K. Sato, L. C. Steinhauer, Y. Tomita, and M. Tuszewski, Fusion Technol. **21**, 2307 (1992).
[8] D. Q. Hwang, M. Ryutova, and H. McLean, Phys. Fluids **6**, 1515 (1999).
[9] R. Raman, F. Martin, B. Quirion, M. St.-Onge, J. L. Lachambre, D. Michaud, B. Sawatzy, J. Thomas, A. Hirose, D. Hwang, N. Richard, C. Cote, G. Abel, D. Pinsonneault, J. L. Gauvreau, B. Stansfield, R. Decoste, A. Cote, W. Zuzak, and C. Boucher, Phys. Rev. Lett. **73**, 3101 (1994).
[10] J. T. Slough and A. L. Hoffman, Phys. Plasmas **6**, 253 (1999).
[11] A. L. Hoffman, P. Gurevich, J. Grossnickle, and J. T. Slough, Fusion Technol. **36**, 109 (1999).
[12] A. Janos, G. W. Hart, C. H. Nam, and M. Yamada, Phys. Fluids **28**, 3667 (1985).
[13] S. C. Hsu and P. M. Bellan, Phys. Plasmas **12**, 032103 (2005).
[14] Y. Ono, M. Inomoto, Y. Ueda, T. Matsuyama, and T. Okazaki, Nucl. Fusion **39**, 2001 (1999).
[15] E. Kawamori and Y. Ono, Phys. Rev. Lett. **95**, 085003 (2005).
[16] M. Yamada, H. P. Furth, W. Hsu, A. Janos, S. Jardin, S. Okbayashi, J. Sinnis, T. H. Stix, and K. Yamazaki, Phys. Rev. Lett. **46**, 188 (1981).
[17] W. C. Turner, G. C. Goldenbaum, E. H. A. Granneman, J. H. Hammer, C. W. Hartman, D. S. Prono, and J. Taska, Phys. Fluids **26**, 1965 (1983).
[18] G. C. Goldenbaum, J. H. Irby, Y. P. Chong, and G. W. Hart, Phys. Rev. Lett. **44**, 393 (1980).
[19] K. Kawai, Z. A. Pietrzyk, and H. T. Hunter, Phys. Fluids **30**, 2561 (1987).
[20] J. C. Fernandez, B. L. Wright, G. J. Marklin, D. A. Platts, and T. R. Jarboe, Phys. Fluids B **1**, 1254 (1989).
[21] T. R. Jarboe, W. T. Hamp, G. J. Marklin, B. A. Nelson, R. G. O'Neill, A. J. Redd, P. E. Seick, R. J. Smith, and J. S. Wrobel, Phys. Rev. Lett. **97**, 115003 (2006).
[22] A. L. Hoffman, H. Y. Guo, K. E. Miller, and R. D. Milroy, Phys. Plasmas **13**, 012507 (2006).
[23] Z. A. Pietrzyk, G. C. Vlases, R. D. Brooks, K. D. Hahn, and R. Raman, Nucl. Fusion **27**, 1478 (1987).
[24] W. F. Pierce, R. J. Maqueda, R. D. Brooks, and R. Farengo, Nucl. Fusion **33**, 117 (1993).
[25] M. Yamada, Y. Ono, H. Hayakawa, M. Katsurai, and F. W. Perkins, Phys. Rev. Lett. **65**, 721 (1990).
[26] M. Yamada, F. W. Perkins, A. K. MacAulay, Y. Ono, and M. Katsurai, Phys. Fluids B **3**, 2379 (1991).
[27] C. D. Cothran, A. Falk, A. Fefferman, M. Landreman, M. R. Brown, and M. J. Schaffer, Phys. Plasmas **10**, 1748 (2003).
[28] S. P. Gerhardt, E. Belova, M. Inomoto, M. Yamada, H. Ji, Y. Ren, and A. Kuritsyn, Phys. Plasmas **13**, 112508 (2006).
[29] S. Nakata, T. Sekiguchi, and M. Isaka, Phys. Fluids **28**, 445 (1985).
[30] S. Nakata, T. Sekiguchi, H. Seki, and K. Yamamoto, Phys. Fluids **29**, 871 (1986).
[31] J. B. Taylor, Phys. Rev. Lett. **33**, 1139 (1974).
[32] J. B. Taylor, Rev. Mod. Phys. **58**, 741 (1986).
[33] G. W. Hart, A. Janos, D. D. Meyerhofer, and M. Yamada, Phys. Fluids **29**, 1994 (1986).
[34] Y. Ono, R. A. Ellis, Jr., A. C. Janos, F. M. Levington, R. M. Mayo, R. W. Motley, Y. Ueda, and M. Yamada, Phys. Rev. Lett. **61**, 2847 (1988).
[35] Y. Ono, M. Yamada, A. C. Janos, and F. M. Levington, Phys. Fluids B **3**, 1452 (1991).
[36] L. C. Steinhauer and A. Ishida, Phys. Rev. Lett. **79**, 3423 (1997).
[37] Z. Yoshida and S. M. Mahajan, Phys. Rev. Lett. **88**, 095001 (2002).
[38] H. Y Guo, A. L. Hoffman, K. E. Miller, and L. C. Steinhauer, Phys. Rev. Lett. **92**, 245001 (2004).
[39] H. Y. Guo, A. L. Hoffman, L. C. Steinhauer, and K. E. Miller, Phys. Rev. Lett. **97**, 235002 (2006).
[40] M. Yamada, H. Ji, S. Hsu, T. Carter, R. Kulsrud, N. Bretz, F. Jobes, Y. Ono, and R. Perkins, Phys. Plasmas **4**, 1936 (1997).
[41] E. Belova, S. C. Jardin, H. Ji, M. Yamada, and R. Kulsrud, Phys. Plasmas **7**, 4996 (2000).
[42] S. P. Gerhardt, E. V. Belova, M. Yamada, H. Ji, M. Inomoto, Y. Ren, and B. McGeehan, Nucl. Fusion **48**, 032001 (2008).
[43] G. W. Hart, C. Chin-Fatt, A. W. DeSilva, G. C. Goldenbaum, R. Hess, and R. S. Shaw, Phys. Rev. Lett. **51**, 1558 (1983).
[44] K. Katyama and M. Katsurai, Phys. Fluids **29**, 1939 (1986).
[45] T. Uyama, Y. Honda, M. Nagata, M. Nishnikawa, A. Ozaki, N. Satimi, and K. Watanabe, Nucl. Fusion **27**, 799 (1987).
[46] C. W. Barnes, T. R. Jarboe, I. Henins, A. R. Sherwood, S. O. Knox, R. Gribble, H. W. Hoida, P. L. Klinger, C. G. Lilliequit, R. K. Linford, D. Platts, R. L. Spencer, and M. Tuszewski, Nucl. Fusion **24**, 267 (1984).
[47] S. O. Knox, C. W. Barnes, G. J. Marklin, T. R. Jarboe, I. Henins, H. W. Hoida, and B. L. Wright, Phys. Rev. Lett. **56**, 842 (1986).
[48] M. G. Rusbridge, S. J. Gee, P. K. Browning, G. C. Cunningham, R. C. Duck, A. al-Karkhy, R. Martin, and J. W. Bradley, Plasma Phys. Controlled Fusion **39**, 683 (1997).
[49] E. B. Hooper, L. D. Pearlstein, and R. H. Bulmer, Nucl. Fusion **39**, 863 (1999).
[50] D. M. Willett, P. K. Browning, S. Woodruff, and K. J. Gibson, Plasma Phys. Controlled Fusion **41**, 595 (1999).
[51] C. T. Holcomb, T. R. Jarboe, D. N. Hill, S. Woodruff, and R. D. Wood, Phys. Plasmas **13**, 022504 (2006).
[52] J. R. Cary, Phys. Fluids **24**, 2239 (1981).
[53] E. V. Belova, S. C. Jardin, H. Ji, M. Yamada, and R. Kulsrud, Phys. Plasmas **8**, 1267 (2001).
[54] E. V. Belova, R. C. Davidson, H. Ji, and M. Yamada, Phys. Plasmas **10**, 2361 (2003).
[55] E. V. Belova, R. C. Davidson, H. Ji, and M. Yamada, Phys. Plasmas **11**, 2523 (2004).
[56] A. Ishida, N. Shibata, and L. C. Steinhauer, Phys. Plasmas **1**, 4022 (1994).
[57] M. N. Rosenbluth and M. N. Bussac, Nucl. Fusion **19**, 489 (1979).
[58] C. Muson, A. Janos, F. Wysocki, and M. Yamada, Phys. Fluids **28**, 1525 (1985).
[59] T. R. Jarboe, I. Henins, H. W. Hoid, R. K. Linford, J. Marshall, D. A. Platts, and A. R. Sherwood, Phys. Rev. Lett. **45**, 1264 (1980).
[60] M. R. Brown, C. D. Cothran, J. Fung, M. Chang, J. Horwitz, M. J. Schaffer, J. Leuer, and E. V. Belova, Phys. Plasmas **13**, 102503 (2006).
[61] P. E. Young, F. J. Wysocki, M. Yamada, and A. Janos, Phys. Fluids B **3**, 2591 (1991).
[62] S. C. Jardin and U. Christensen, Nucl. Fusion **21**, 1665 (1981).
[63] S. C. Jardin, M. S. Chance, R. L. Dewar, R. C. Grimm, and D. A. Monticello, Nucl. Fusion **21**, 1203 (1981).
[64] H. Ji, M. Yamada, R. Kulsrud, N. Pomphrey, and H. Himura, Phys. Plasmas **5**, 3685 (1998).
[65] A. Bondeson, G. Marklin, Z. G. An, H. H. Chen, Y. C. Lee, and C. S. Lium, Phys. Fluids **24**, 1682 (1981).
[66] S. P. Gerhardt, E. V. Belova, M. Yamada, H. Ji, M. Inomoto, Y. Ren, and B. McGeehan, Phys. Rev. Lett. **99**, 245004 (2007).
[67] S. P. Gerhardt, E. V. Belova, M. Yamada, H. Ji, M. Inomoto, C. M. Jacobson, R. Maqueda, B. McGeehan, and Y. Ren, Phys. Plasmas **15**, 022503 (2008).
[68] M. K. Bevir and J. W. Grey, in Proceedings of the Reversed-Field Pinch Theory Workshop, Los Alamos, 1981, Report No. LA-8944-C.
[69] J. K. Anderson, C. B. Forest, T. M. Biewer, J. S. Sarff, and J. C. Wright, Nucl. Fusion **44**, 162 (2004).
[70] K. F. Schoenberg, R. W. Moses, Jr., and R. Hagenson, Phys. Fluids **27**, 1671 (1984).

[71]L. Spitzer, *The Physics of Fully Ionized Gases* (Interscience, New York, 1962).
[72]A. Kuritsyn, M. Yamada, S. P. Gerhardt, H. Ji, R. Kulsrud, and Y. Ren, Phys. Plasmas **13**, 055793 (2006).
[73]F. Trintouk, M. Yamada, H. Ji, R. M. Kulsrud, and T. A. Carter, Phys. Plasmas **10**, 319 (2003).
[74]K. Miyamoto, *Plasma Physics For Nuclear Fusion* (MIT, Cambridge, 1989).
[75]SPIRIT stands for Self-organized Plasma with Induction, Reconnection, and Injection Techniques.
[76]M. Yamada, H. Ji, S. P. Gerhardt, E. V. Belova, R. C. Davidson, and D. R. Mikkelsen, J. Plasma Fusion Res. **2**, 004 (2007).
[77]Y. Ono, M. Yamada, T. Akao, T. Tajima, and R. Matsumoto, Phys. Rev. Lett. **76**, 3328 (1996).
[78]T. R. Jarboe, C. W. Barnes, I. Henins, H. W. Hoida, S. O. Knox, R. K. Linford, and A. R. Sherwood, Phys. Fluids **27**, 13 (1984).
[79]U. Shumlack and C. W. Hartman, Phys. Rev. Lett. **75**, 3285 (1995).
[80]U. Shumlack, R. P. Golingo, B. A. Nelson, and D. J. Den Hartog, Phys. Rev. Lett. **87**, 205005 (2001).
[81]M. N. Rosenbluth, N. A. Krall, and N. Rostoker, Nucl. Fusion Suppl. Part I, 143 (1962).

The Princeton Plasma Physics Laboratory is operated
by Princeton University under contract
with the U.S. Department of Energy.

Information Services
Princeton Plasma Physics Laboratory
P.O. Box 451
Princeton, NJ 08543

Phone: 609-243-2750
Fax: 609-243-2751
e-mail: pppl_info@pppl.gov
Internet Address: http://www.pppl.gov